Check for updates

The KSHV ORF20 Protein Interacts with the Viral Processivity Factor ORF59 and Promotes Viral Reactivation

D. Hoffman,[a] W. Rodriguez,[a] D. Macveigh-Fierro,[a] J. Miles,[a] (ORCID) M. Muller[a]

[a]Microbiology Department, University of Massachusetts Amherst, Amherst, Massachusetts, USA

ABSTRACT Upon Kaposi's Sarcoma-associated herpesvirus (KSHV) lytic reactivation, rapid and widespread amplification of viral DNA (vDNA) triggers significant nuclear reorganization. As part of this striking shift in nuclear architecture, viral replication compartments are formed as sites of lytic vDNA production along with remarkable spatial remodeling and the relocalization of cellular and viral proteins. These viral replication compartments house several lytic gene products that coordinate viral gene expression, vDNA replication, and nucleocapsid assembly. The viral proteins and mechanisms that regulate this overhaul of the nuclear landscape during KSHV replication remain largely unknown. KSHV's *ORF20* is a widely conserved lytic gene among all herpesviruses, suggesting it may have a fundamental contribution to the progression of herpesviral infection. Here, we utilized a promiscuous biotin ligase proximity labeling method to identify the proximal interactome of ORF20, which includes several replication-associated viral proteins, one of which is ORF59, the KSHV DNA processivity factor. Using coimmunoprecipitation and immunofluorescence assays, we confirmed the interaction between ORF20 and ORF59 and tracked the localization of both proteins to KSHV replication compartments. To further characterize the function of ORF20, we generated an ORF20-deficient KSHV and compared its replicative fitness to that of wild-type virus. Virion production was significantly diminished in the ORF20-deficient virus as observed by supernatant transfer assays. Additionally, we tied this defect in viable virion formation to a reduction in viral late gene expression. Lastly, we observed an overall reduction in vDNA replication in the ORF20-deficient virus, implying a key role for ORF20 in the regulation of lytic replication. Taken together, these results capture the essential role of KSHV ORF20 in progressing viral lytic infection by regulating vDNA replication alongside other crucial lytic proteins within KSHV replication compartments.

IMPORTANCE Kaposi's Sarcoma-associated herpesvirus (KSHV) is a herpesvirus that induces lifelong infection, and as such, its lytic replication is carefully controlled to allow for efficient dissemination from its long-term reservoir and for the spread of the virus to new hosts. Viral DNA replication involves many host and viral proteins, coordinating both in time and space to successfully progress through the viral life cycle. Yet, this process is still not fully understood. We investigated the role of the poorly characterized viral protein ORF20, and through proximity labeling, we found that ORF20 interacts with ORF59 in replication compartments and affects DNA replication and subsequent steps of the late viral life cycle. Collectively, these results provide insights into the possible contribution of ORF20 to the complex lytic DNA replication process and suggest that this highly conserved protein may be an important modulator of this key viral mechanism.

KEYWORDS DNA replication, Kaposi's sarcoma-associated herpesvirus, herpesviruses

Human herpesvirus 8, also known as Kaposi's Sarcoma-associated herpesvirus (KSHV), is an oncogenic virus that has the incredible ability of initiating and

maintaining lifelong infections in its host (1). In immunocompromised individuals, these lifelong infections can lead to the development of several malignancies, including Kaposi's sarcoma (KS), primary effusion lymphoma (PEL), and multicentric Castleman disease (MCD) (2–4). Similar to other herpesviruses, KSHV undergoes a biphasic life cycle that features both latent and lytic phases (1). During latency, KSHV can persist for decades within its infected host, during which time only a few viral proteins are expressed. These latency-associated proteins in concert with host machinery coordinate viral genome maintenance and replication while evading detection by host immune surveillance. However, upon reactivation into the lytic phase, the vast majority of KSHV genes are expressed in an ordered cascade, rapidly amplifying the viral genome and triggering the assembly of new viral particles. As with other herpesviruses, KSHV lytic phase replication progresses via a mechanism distinct from that of latent viral DNA replication (5). In particular, lytic replication initiates at a different origin of replication (ori-Lyt) on the viral genome and does not occur in synchrony with the host cell (6, 7). Instead, KSHV lytic replication requires at least eight viral proteins (ORF9, ORF6, ORF40, ORF44, ORF56, ORF50, ORF59, and ORFK8), including its own virally encoded DNA polymerase (ORF9) (1, 8, 9) and DNA polymerase processivity factor (ORF59) (10–12). In particular, ORF59 has been shown to be recruited to the lytic origin of replication via its binding to ORF50 (RTA) (13), which leads to the recruitment of the viral DNA polymerase and initiation of replication (10, 11, 14). Therefore, KSHV lytic DNA replication is reliant on the recruitment of ORF59 and the assembly of a replication complex composed of multiple viral lytic factors.

To accommodate the large-scale amplification of the viral genome, lytic replication is accompanied by a drastic reorganization of the nucleus. This results in major nuclear and nucleolar remodeling, including relocalization of host chromatin and displacement of several host proteins such as nucleolin and nucleophosmin (15). This represents one of the hallmarks of herpesvirus replication: the formation of a "bean-shaped" viral replication compartment (RC) (16–19).

Among the ~85 viral proteins encoded by the KSHV genome, ORF20 belongs to the herpesviral core *UL24* gene family, widely conserved throughout the *Alpha-*, *Beta-*, and *Gammaherpesvirinae* (20, 21). Very little is known about the functions of KSHV ORF20 and its orthologs across the herpesvirus family. For ORF20 orthologs harbored by HSV-1 (UL24), human cytomegalovirus (HCMV) (UL76), and murine gammaherpesvirus 68 (MHV68) (ORF20), each have been reported to modulate cell cycle arrest and apoptosis (22–24). Past studies have also shown that KSHV ORF20 and its orthologs UL24 and UL76 localize to the nucleoli of transfected cells (25–27) with a demonstrably complex localization pattern (28). Furthermore, UL24 was shown to contribute to nucleolar reorganization by affecting the expression pattern of key nucleolar proteins (25, 29–31). ORF20 mRNA expression kinetics seem to vary depending on the host cell, demonstrating late gene kinetics upon *de novo* infection of primary human umbilical vein endothelial cells (HUVEC) and upon reactivation of a latently infected body cavity-based lymphoma cell line (BCBL1) (32). However, more recently, upon lytic reactivation in endothelial cells, KSHV *ORF20* was shown to be expressed as an immediate early viral gene (28). It was also demonstrated that through its interaction with oligoadenylate synthetase-like protein (OASL), ORF20 enhances KSHV replication, possibly by regulating ribosome composition (28). Given that ORF20 is widely conserved in the herpesvirus family and based on these roles gathered from several herpesvirus members, we set out to investigate the role of ORF20 in KSHV and whether its function could bridge these observations of both nuclear remodeling and high conservation.

Here, we investigated the ORF20 microenvironment by proximity labeling using BioID and identified ORF59 as an ORF20 interactor. We then tracked the localization of ORF20 upon lytic reactivation and found it localizes to KSHV replication compartments, where it colocalizes with ORF59. Furthermore, we found that cells infected with an ORF20-deficient virus have a severe defect in viral DNA replication, late gene expression, and subsequent virion formation. Taken together, our results indicate that ORF20
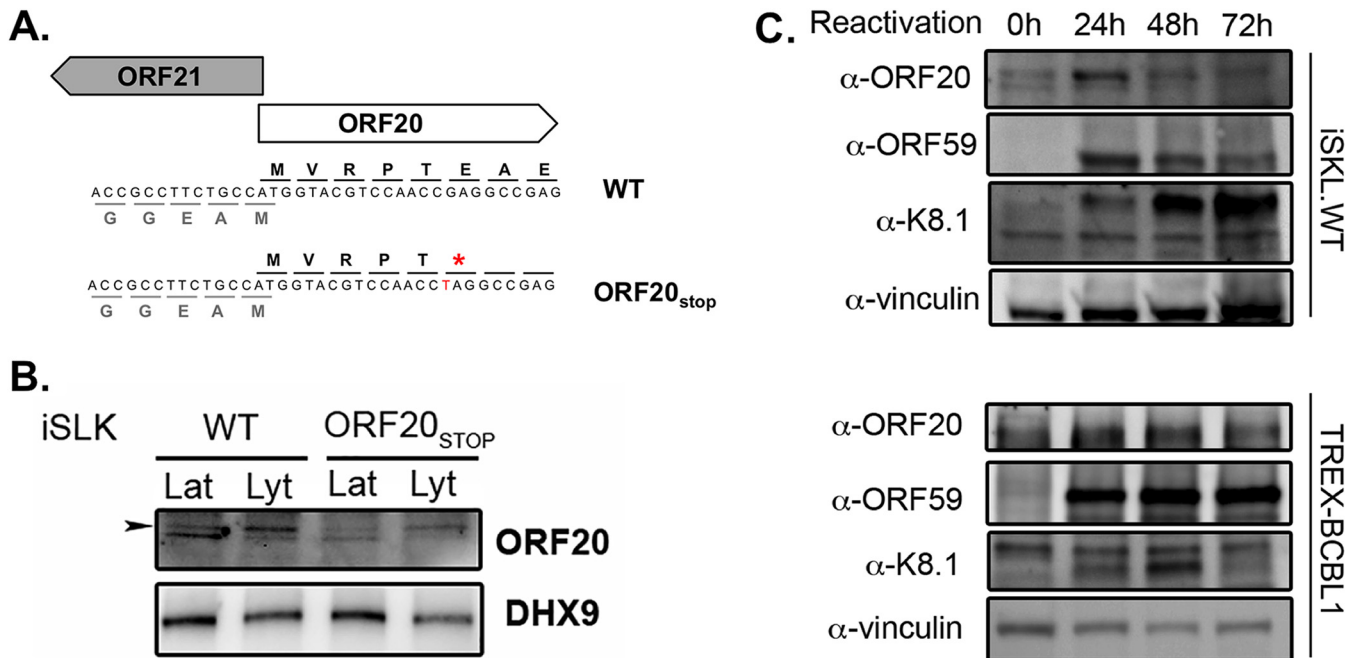
FIG 1 Characterization of the expression of KSHV ORF20. (A) Diagram showing the genomic locus of *ORF20*, with surrounding gene *ORF21*, depicting the location of the introduced mutation. (B) ORF20 expression was assessed by Western blotting in both iSLK.WT and ORF20STOP cells whether in their latent phase (Lat) or lytic phase (Lyt). DHX9 served as a loading control. (C) Western blot showing the expression kinetics of ORF20 in iSLK.WT cells (top) and TREX-BCBL1 cells (bottom) after reactivation with doxycycline and sodium butyrate for the indicated times. ORF59 (early kinetic) and K8.1 (late kinetic) expression is shown as controls. Vinculin served as a loading control.

is an important regulator of the KSHV lytic cycle. By placing ORF20 at the replication compartment where it interacts with KSHV processivity factor ORF59, our work supports a role for ORF20 in KSHV complex lytic DNA replication.

RESULTS

KSHV ORF20 proximal proteome identifies novel ORF20 interactors. To better understand the function of ORF20 during lytic KSHV infection, we used the proximity labeling method BioID to characterize the ORF20 microenvironment. We first generated an ORF20-deficient virus (ORF20$_{STOP}$) using the BAC16 Red recombinase system (33) by mutating the *ORF20* genomic sequence 16 nucleotides downstream of its translation start site (Fig. 1A). This mutation resulted in the expression of a premature termination codon. This virus was used to establish a latently infected cell line in iSLK cells that are here referred to as iSLK-ORF20$_{STOP}$. Using a newly generated ORF20 antibody, we confirmed that ORF20 expression is abrogated in these cells (Fig. 1B). Because the timing of ORF20 expression is crucial to set our experimental timeline, and due to expression being previously inconsistent, we next tested when endogenous ORF20 was made in iSLK.WT cells, a KSHV-positive cell line similar to the one used to establish our ORF20-deficient viral mutant. Based on observations of ORF20 expression in iSLK.WT cells relative to that in the ORF20$_{STOP}$ cells, the band corresponding to ORF20 is the upper band in the doublet detected with this antibody (Fig. 1B). ORF20 was previously shown to express several isoforms, it is thus possible that these band doublets detected here represent two different isoforms. We further explored the kinetic expression of ORF20 in these cells and detected a peak of ORF20 expression as soon as 24 h post-lytic reactivation (Fig. 1C). This is similar to the expression of ORF59, a KSHV early gene, but much earlier than K8.1, a KSHV late gene. Based on this pattern, ORF20 can be considered an early gene in these cells as was recently reported (28). We also investigated its expression in TREX-BCBL1 cells, a KSHV-positive B cell line. In these cells, expression of ORF20 was faint, and we no longer detected the doublet observed in iSLK cells, possibly suggesting that only one isoform is expressed in these cells. Here,

we also detected expression at 24 h postreactivation; however, as opposed to that in iSLK cells, its expression was stable at 48 h, highlighting a possible cell-specific regulation of ORF20 expression.

To investigate the ORF20 proximal interactome, we used the proximity labeling method BioID in which a promiscuous biotin ligase—BirA—is fused to the protein of interest. Biotinylated proteins resulting from the action of this BirA ligase can then be selectively isolated and identified by mass spectrometry (34). We thus generated a plasmid in which the $BirA_{R118G}$ biotin ligase was fused at the C terminus of ORF20, which was subsequently used to rescue ORF20 expression in the iSLK-ORF20$_{STOP}$ cells. This setup was used to identify novel ORF20 direct and indirect interactors. iSLK-ORF20$_{STOP}$ cells were reactivated for 24 h with doxycycline and sodium butyrate to trigger KSHV lytic cycle and transfected with BirA-ORF20 (or mock transfected) with excess biotin added to the medium at the time of transfection. After 16 h, cells were lysed, and streptavidin-conjugated beads were used to isolate biotinylated proteins. After verifying the expression of our BirA-ORF20-hemagglutinin (HA) construct by Western blotting, the identity of the biotinylated proteins was determined by liquid chromatography-tandem mass spectrometry (LC-MS/MS) (Fig. 2A). As shown in Table S1 in the supplemental material, after filtering, we identified 316 high-confidence unique proteins in the ORF20 microenvironment, of which, 62 were previously identified with KSHV ORF20 (28). Based on gene ontology (GO) term analysis on ORF20 interactors, several functional categories emerged, including several related to ribosomal regulation, as previously reported (Fig. 2B). Intriguingly, several categories placed ORF20 at the nucleosome and close to proteins regulating helicase activity. Moreover, we detected ORF59, the KSHV lytic DNA processivity factor, which we decided to explore further.

KSHV ORF20 interacts with ORF59 and localizes to the replication compartment. To validate the interaction between ORF20 and ORF59 detected by BioID, we used coimmunoprecipitation (Co-IP). We first coexpressed ORF20 and ORF59 in HEK293T cells and confirmed the interaction observed in our BirA experiment (Fig. 3A). Furthermore, we tested the interaction directly in the KSHV-positive cell line iSLK.WT. Cell lysates were collected from iSLK.WT cells in either their latent or reactivated state when both ORF59 and ORF20 should be expressed. We immunoprecipitated ORF59 overnight and immunoblotted the eluates. We found that ORF59 and ORF20 interact during KSHV lytic phase (Fig. 3B).

ORF59 has a distinctive subcellular localization during KSHV lytic cycle and localizes to replication compartments. These replication compartments are the site of the viral genome replication and are easily identifiable as dark areas in 4′,6-diamidino-2-phenylindole (DAPI) staining of host nuclei. Given that ORF20 was previously shown to localize to discrete nuclear foci, we hypothesized that ORF20 could colocalize with ORF59 at these RCs. We first investigated if we could detect a fraction of ORF20 in the RC in reactivated iSLK cells by immunofluorescence assay (IFA). In iSLK.WT cells transfected with Flag-ORF20, ORF20 expression was predominantly nuclear and distinctively present in nuclear puncta overlapping DAPI-negative areas. Because, in iSLK.WT cells, endogenous viral ORF20 expression may interfere with our Flag-tagged construct, we confirmed this expression pattern in iSLK.ORF20$_{STOP}$ cells, where we also found ORF20 expressed in DAPI-negative areas of the nucleus (Fig. 3C). Since this expression pattern is consistent with ORF59 localization patterns and our BioID and Co-IP indicate an interaction between ORF59 and ORF20, we next monitored the localization of both ORF59 and ORF20. To do so, we used the KSHV-positive TREX-BCBL1 cells, since they do not have any fluorescent marker and thus allowed us to use an additional color channel. In these cells, ORF59 and ORF20 appear to colocalize in the nucleus in areas reminiscent of replication compartments (Fig. 3C).

KSHV lacking ORF20 shows defects in virion formation and late gene expression. Given that ORF20 function is poorly understood, we next wanted to better define its role during the KSHV lytic cycle. Based on our data, ORF20 is expressed early in the lytic cycle and is expressed in RCs where it interacts with ORF59. Moreover, ORF20 is very well conserved in the herpesvirus family, suggesting that its function might be crucial
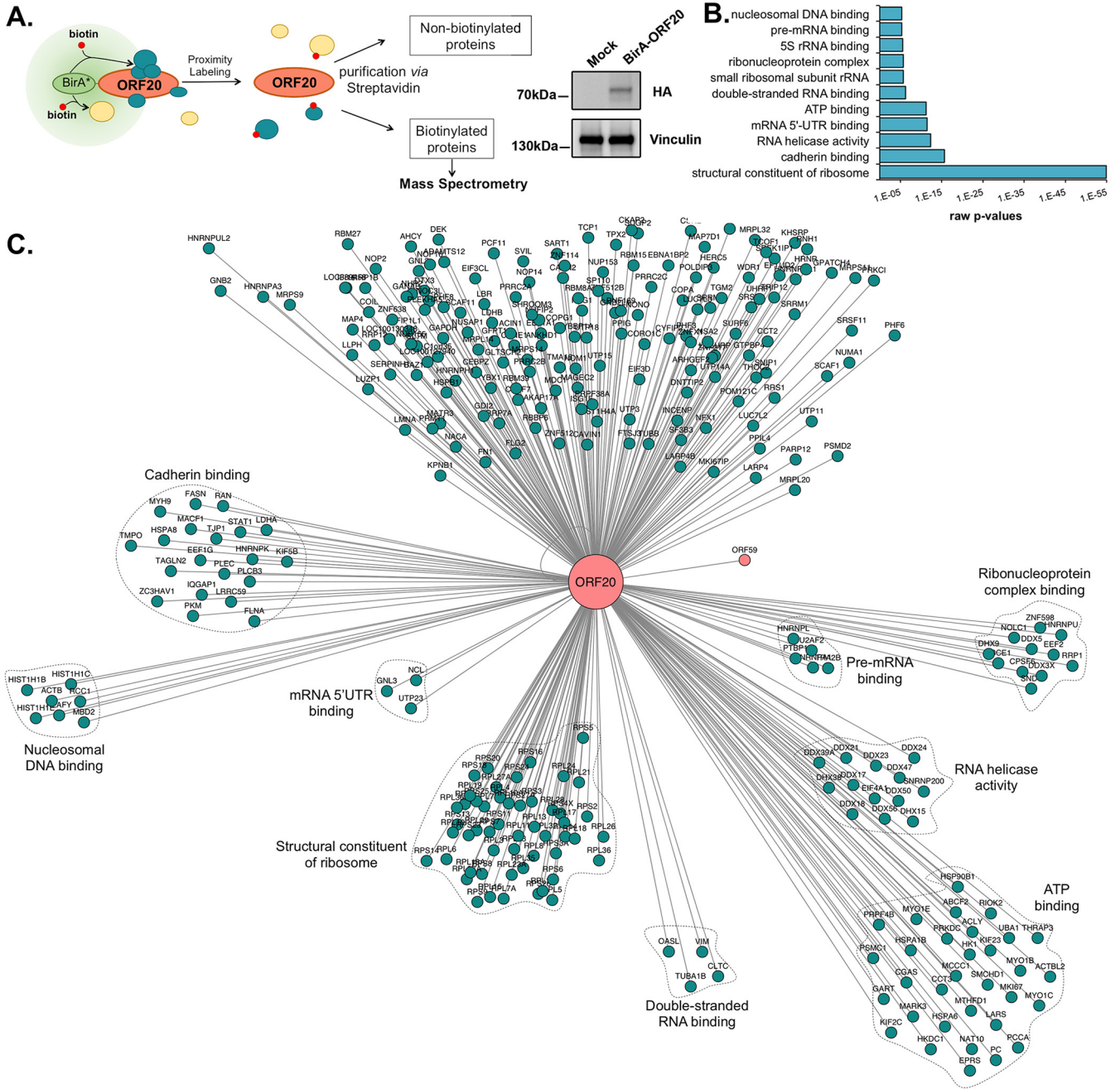
FIG 2 Determination of ORF20 proximal interactome. (A) Schematic representation of the BioID assay, where ORF20 is fused to the biotin ligase BirA which will transfer a biotin to proteins coming in close proximity to ORF20. Expression of the BirA-ORF20 fusion is shown on the right. Vinculin serves as a loading control (B) iSLK.ORF20$_{STOP}$ cells were transfected with ORF20-BirA and subjected to BioID and mass spectrometry. The bar graph represents the top GO terms associated with ORF20 interacting partners, and the network, generated by Cytoscape, represents the ORF20 proximal interactome. Proteins annotated in the categories highlighted in the bar graph are shown in clusters.

for proper progression of viral infection, and so we hypothesized that ORF20 could be important for the regulation of viral replication. To address this question, we first monitored the ability of the iSLK.ORF20$_{STOP}$ cells to produce progeny virions by supernatant transfer assay and showed that, compared to iSLK.WT cells, these almost completely failed to produce any viable virions (Fig. 4B and C). When ORF20 expression was rescued using ectopic expression of our HA-tagged ORF20 plasmid, virion production was restored, suggesting that the defect observed in these cells is caused by the lack of ORF20 expression.
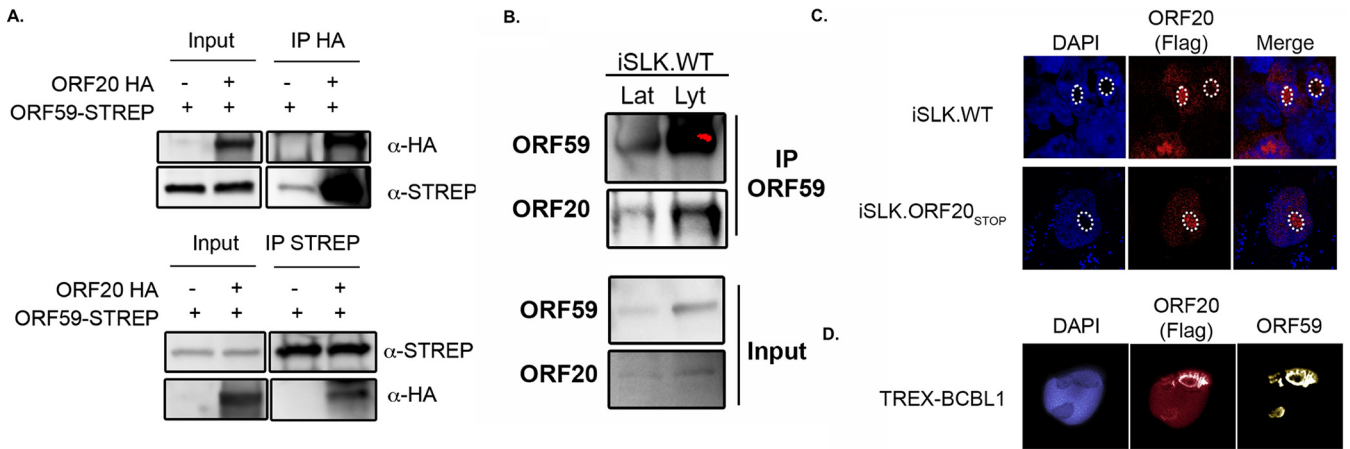
FIG 3 ORF20 interacts and colocalizes with ORF59 in KSHV replication compartments. (A) HEK293T cells were transiently transfected with HA-ORF20 (or mock) and streptavidin (strep)-ORF59 as indicated, and a co-IP was performed using anti-HA antibody. Reverse Co-IP was performed using anti-strep antibody. (B) Lysates of latently infected (Lat) or doxycycline (DOX)-reactivated (Lyt) KSHV-positive iSLK.WT cells were subjected to IP with an anti-ORF59 antibody, and then Western blotted (WB) for ORF20 or ORF59. (C) Reactivated KSHV-positive iSLK.WT or iSLK.ORF20$_{STOP}$ cells were transfected with Flag-ORF20 and, 24 h later, were subjected to immunofluorescence assay using an anti-Flag antibody (red) and DAPI staining to identify nuclei (blue). White dotted circles denote DAPI-deficient nuclear domain representing KSHV replication compartments. (D) DOX-, TPA-, and ionomycin (iono)-treated KSHV-positive TREX-BCBL1 cells were transfected with Flag-ORF20 and, 24 h, later subjected to immunofluorescence assay using an anti-Flag antibody (red), anti-ORF59 antibody (yellow), and DAPI staining to identify nuclei (blue).

Provided that the ORF20$_{STOP}$ cells were severely deficient in virion production, we next investigated whether ORF20 expression, or lack thereof, influences viral gene expression. We investigated the expression kinetics of two viral genes for which we have antibodies: the early viral protein ORF59 and the late major capsid protein K8.1. iSLK.WT or iSLK.ORF20$_{STOP}$ cells were reactivated, and either total RNA was extracted and used for reverse-transcription quantitative PCR (RT-qPCR) or cell lysates were collected and used for immunoblotting. Compared with iSLK.WT cells, iSLK.ORF20$_{STOP}$ cells displayed a drastic reduction of K8.1 expression both at the RNA (Fig. 5A) and protein (Fig. 5B) levels but only a marginal effect on ORF59. Because of this differential effect on early (ORF59) versus late (K8.1) gene expression and because ORF20 appears to be expressed in replication compartments, we hypothesized that ORF20 could have an impact on KSHV DNA replication. Therefore, we next quantified this process in both iSLK.WT cells and iSLK.ORF20$_{STOP}$ cells. We observed a reduction in viral DNA replication in cells lacking ORF20 expression, which was rescued by ectopic expression of ORF20 (Fig. 5C). This suggests that the presence of ORF20 is required for proper progression of KSHV DNA replication and, consequently, late gene expression and viable virion production.
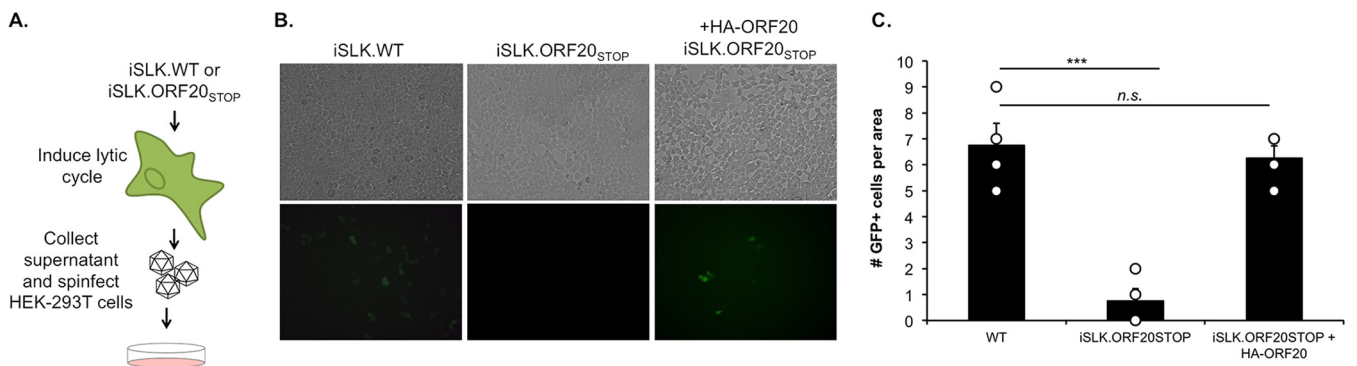

FIG 4 Lack of ORF20 reduces virion production. (A) Diagram depicting the supernatant transfer assay in iSLK cells. (B) Supernatant transfer assay was used as a proxy for virion production and performed as described in panel A. Infection of live HEK293T cells was monitored by contrast (top) and green fluorescent protein (GFP) imaging (bottom) on a fluorescence microscope. (C) Quantification of GFP-positive cells using ImageJ. Values represent four independent views of the infected cells.
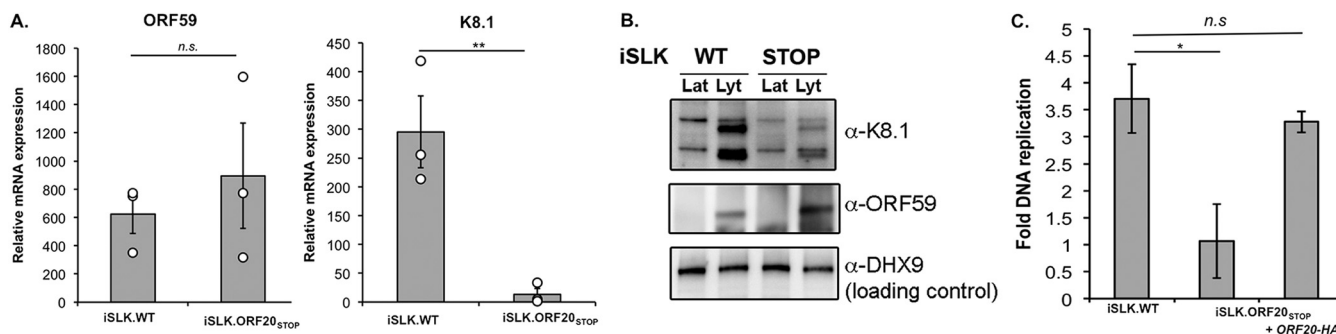
FIG 5 ORF20 is involved in regulating DNA replication and subsequent late gene expression. (A and B) Total RNA was extracted from unreactivated and reactivated iSLK.WT or iSLK.ORF20$_{STOP}$ cells. (A) RNA was then subjected to RT-qPCR to quantify expression of the indicated viral genes. Bars represent the relative mRNA fold change over that in unreactivated cells. (B) Western blot showing the expression of ORF59 and K8.1 in iSLK.WT or iSLK.ORF20$_{STOP}$ cells after reactivation with doxycycline and sodium butyrate. DHX9 served as a loading control. (C) DNA replication was measured by qPCR of the viral genome before and after reactivation of the lytic cycle iSLK.WT or iSLK.ORF20$_{STOP}$ cells. ORF20 expression was complemented by exogenous expression of ORF20-HA (right bar).

DISCUSSION

In this study, we demonstrate that KSHV ORF20 localizes to replication compartments where it interacts with KSHV DNA replication processivity factor ORF59. Our approach to better define the contribution of ORF20 to KSHV lytic replication was to investigate the ORF20 microenvironment by proximity labeling. Namely, we used BioID to uncover ORF20 proximal interacting partners, complementing past work conducted to reveal the interactome of ORF20 (28). We confirmed many of the previously identified ORF20 protein partners, including many ribosomal factors as well as OASL, as was previously reported (28). The interaction between ORF20 and OASL has actually been extensively characterized, and given the known roles of OASL in interferon regulation and antiviral immunity, it would be interesting to investigate whether its interaction with ORF20 affects the viral life cycle that we detected in this study (35). In addition, our approach includes not only direct interaction but also transient interactions and a close proximity factor and therefore greatly expands the scope of ORF20 potential partners.

A GO term analysis of the ORF20 microenvironment also revealed several novel putative functions for ORF20, with many relating to RNA binding. Since ORF20 was previously hypothesized to help bridge specific mRNAs to polysomes (28), it would be interesting to further investigate this aspect of ORF20 biology. In addition, nucleolin (NCL) was identified to be in close proximity to ORF20, which is intriguing, since ORF20 ortholog UL24 in HSV-1 was shown to be directly involved in the dispersal of NCL during infection (29). This suggests that this dispersal, which is also observed during KSHV infection (36, 37), might be a conserved function of ORF20.

We also show that ORF20 has a distinctive subcellular localization that we identified is in replication compartments. Of note, we also noticed that ORF20 subcellular localization was heterogeneous, and we observed that ORF20 could also be more diffuse in the nucleus dependent on experimental timing. This has been reported before (38) and suggests that ORF20 localization might be highly dynamic and only transiently needed at the replication compartment.

Replication compartments are enriched for many host and viral proteins involved in lytic DNA replication that shuttle in and out depending on their function during this process (35, 39). The formation of replication compartments is a complex but common process for viruses: these membraneless compartments grow and coalesce over infection, using liquid-liquid phase separation and pushing host chromatin to the nuclear periphery (40–42). Replication compartments are the site for viral genome replication, transcription, and packaging (19). Finding ORF20 at this site thus brings up an important question: is ORF20 involved in KSHV DNA replication? Past work on ORF20 orthologs has suggested that this viral protein is important for viral replication (43), yet the precise mechanism is still unclear. However, the ORF20 ortholog in MHV68 was not

classified as an essential viral gene (44), suggesting that ORF20 contribution to DNA replication might vary slightly among the various herpesviruses.

One particularity of ORF20 is that it harbors a conserved PD-(D/E)XK endonuclease domain (45, 46). This signature nuclease domain is found in a number of proteins that can cleave nucleic acids. The other known KSHV PD-(D/E)XK nuclease is the viral protein SOX, which is responsible for host shutoff during the lytic phase (47–49). It is thus interesting to note that a second viral nuclease is harbored by KSHV, and since we are placing ORF20 in the replication compartment, this nuclease activity could be important for DNA replication. The DNase activity of SOX was previously hypothesized to be responsible for initiating DNA replication when a viral endonuclease is needed to create a nick in the origin of replication. However, this could never be proven, and instead, SOX DNase activity was shown to be important for branch resolution during replication (50). Similarly, in HSV-1, SOX ortholog UL12 was demonstrated to be involved in recombination (51) but has not yet been shown to be the nickase necessary for rolling circle replication initiation. This therefore leaves open the question of which protein—viral or cellular—carries out this single-stranded cleavage at the origin of replication during herpesviruses lytic replication. It would be interesting to test whether the ORF20 PD-(D/E)XK domain is functional and whether this viral protein contributes to this process.

Like that of other herpesviruses, KSHV lytic DNA replication is distinct from latent viral DNA replication, both because it uses a specific lytic origin of replication and because KSHV relies on viral and not cellular factors to regulate this process. Regulation of this process is complex and extensive; more work is necessary to fully understand this crucial viral mechanism. As we understand more and more about these previously uncharacterized viral proteins, such as ORF20, we are getting closer to this goal. Given the frequently multifunctional roles of viral proteins, it will be of interest to also explore possible additional activities of ORF20, including how it may contribute to nuclear remodeling during KSHV replication and whether ORF20 has an intrinsic nuclease activity.

MATERIALS AND METHODS

Cells and transfections. HEK293T cells (ATCC) were grown in Dulbecco's modified Eagle medium (DMEM; Invitrogen) supplemented with 10% fetal bovine serum (FBS). The KSHV-infected renal carcinoma human cell line iSLK.BAC16 (52) (kind gift from B. A. Glaunsinger) bearing doxycycline-inducible RTA was grown in DMEM supplemented with 10% FBS. For reactivation, BAC16-containing iSLK cells were treated with 1 μg/ml doxycycline and 1 mM sodium butyrate for the designated times. The KSHV-positive B cell line bearing a doxycycline-inducible version of the major lytic transactivator RTA (TREX-BCBL1) (53) was maintained in RPMI medium (Invitrogen) supplemented with 10% FBS (Invitrogen), 200 μM L-glutamine (Invitrogen), 100 U/ml penicillin-streptomycin (Invitrogen), and 50 μg/ml hygromycin B (Omega Scientific). Lytic reactivation was induced by treatment with 20 ng/ml 2-O-tetradecanoyl-phorbol-13-acetate (TPA; Sigma), 1 μg/ml doxycycline (BD Biosciences), and 500 ng/ml ionomycin (Fisher Scientific) for 48 h.

The KSHV ORF20 premature stop codon (ORF20$_{STOP}$) mutant was engineered using the scarless Red recombination system in BAC16 GS1783 *Escherichia coli* as previously described (52), except using two gBlocks (IDT) to introduce the mutation. Each gBlock contained half of the kanamycin resistance cassette, as well as the desired mutation, and was joined by short overlap extension PCR before being used as the linear insert in the established protocol. The BAC16 ORF20 mutant was purified using the NucleoBond BAC 100 kit (Clontech). iSLK cell lines latently infected with the KSHV ORF20$_{STOP}$ virus were then established by coculture; HEK293T cells were transfected with 5 μg of ORF20$_{STOP}$ BAC DNA. The following day, the cells were trypsinized and mixed 1:1 with the KSHV-negative iSLK-puro cells and then treated with 25 nM 12-O-tetradecanoylphorbol-13-acetate (TPA) and 300 nM sodium butyrate for 4 days to induce lytic replication. iSLK cells were then selected using selection medium containing 300 μg/ml hygromycin B, 1 μg/ml puromycin, and 250 μg/ml G418. The medium was replaced every other day for ~2 weeks, gradually increasing the hygromycin B concentration until there were no HEK293T cells remaining. These cells are here referred to as iSLK-ORF20$_{STOP}$.

For DNA transfections, cells were plated and transfected after 24 h when 70% confluent using PolyJet (SignaGen).

Supernatant transfers were carried out in iSLK cells. The cells were reactivated for 48 h, and then the supernatants from induced iSLK cells were syringe filtered through a 0.45-μm-pore-size filter and spinfected into HEK293T cells at 1,500 rpm for 1.5 h at 37°C. Twenty-four hours later, cells were imaged on a fluorescence microscope.

Plasmids. The KSHV ORF20 open reading frame (ORF) was obtained from the KSHV ORFeome (54) and cloned into a pcDNA4 Nter-3×Flag vector. For the BirA-ORF20 construct, the sequence of the BirA ligase (containing a mutation [R118G] allowing it to act as a promiscuous biotin ligase) was PCR amplified from pcDNA3.1 MCS-BirA(R118G)-HA and cloned at the C terminus of ORF20 in the pcDNA4 Nter-3-×Flag vector. All cloning steps were performed using in-fusion cloning (Clontech-TaKaRa) and were verified by Sanger sequencing.

RT-qPCR. Total RNA was harvested using TRIzol according to the manufacture's protocol. cDNAs were synthesized from 1 μg of total RNA using avian myeloblastosis virus (AMV) reverse transcriptase (Promega) and used directly for quantitative PCR (qPCR) analysis with the SYBR green qPCR kit (Bio-Rad) on a QuantStudio 3 real-time PCR machine. Signals obtained by qPCR were normalized to those of 18S. For DNA replication calculation, iSLK cells were incubated with 5× proteinase K digestion buffer (50 mM Tris-HCl [pH 7.4], 500 mM NaCl, 5 mM EDTA, 2.5% SDS) and digested with proteinase K (80 μg/ml) overnight at 55°C. The genomic DNA (gDNA) was isolated by using a Zymo Quick gDNA miniprep kit according to the manufacturer's instructions. DNA levels were quantified using relative standard curves with primers specific for KSHV *ORF59* (5′-AATCCACAGGCATGATTGC-3′ and 5′-CACACTTCCACCTCCCCTAA-3′) or a region in the *GAPDH* promoter (5′-TACTAGCGGTTTTACGGGCG-3′ and 5′-TCGAACAGGAGGAGCAGAGAGCGA-3′). The relative genome numbers were normalized to *GAPDH* to account for loading differences and to uninduced samples to account for the starting genome copy number.

Western blotting. Cell lysates were prepared in lysis buffer (150 mM NaCl, 50 mM Tris, 0.5% NP-40, 1 mM dithiothreitol [DTT], and protease inhibitor tablets) and quantified by Bradford assay. Equivalent amounts of each sample were resolved by SDS-PAGE and Western blotted with the following antibodies at 1:1,000 in TBST (Tris-buffered saline, 0.1% Tween 20): rabbit anti-ORF20 (Yenzym) rabbit anti-DHX9/RNA helicase A (Abcam), rabbit anti-glyceraldehyde-3-phosphate dehydrogenase (GAPDH) (Abcam), rabbit anti-vinculin (Abcam), and rabbit anti-HA (Abcam) antibodies. The rabbit anti-ORF59 and anti-K8.1 antibodies were used at 1:10,000 and 1:50,000, respectively, and were a gift from the Glaunsinger lab. Primary antibody incubations were followed by horseradish peroxidase (HRP)-conjugated goat anti-mouse or goat anti-rabbit secondary antibodies (Southern Biotechnology, 1:5,000).

Immunoprecipitation. Cells were lysed in low-salt lysis buffer (150 mM NaCl, 0.5% NP-40, 50 mM Tris [pH 8], 1 mM DTT, and protease inhibitor cocktail), and protein concentrations were determined by Bradford assay. Equivalent quantities of each sample and at least 400 μg of total protein were incubated overnight with the designated antibody and then with protein G-coupled magnetic beads (Life Technologies) for 1 h. Beads were washed extensively with lysis buffer. Samples were resuspended in Western blot loading buffer before resolution by SDS-PAGE.

Immunofluorescence assays. iSLK-ORF20$_{STOP}$ or TREX-BCBL1 cells were grown on coverslips and fixed in 4% formaldehyde for 20 min at room temperature. Cells were then permeabilized in 1% Triton X-100 and 0.1% sodium citrate in phosphate-buffered saline (PBS) for 10 min, saturated in bovine serum albumin (BSA) for 30 min, and incubated with the designated antibodies at a 1:100 dilution. After 1 h, coverslips were washed in PBS and incubated with Alexa Fluor 594 or Alexa Fluor 488 secondary antibodies at 1:1,500 (Invitrogen). Coverslips were washed again in PBS and mounted in DAPI-containing Vectashield mounting medium (Vector Labs) to stain cell nuclei before visualization by confocal microscopy on a Nikon A1 resonant scanning confocal microscope (A1R-SIMe). The microscopy data were gathered in the Light Microscopy Facility and Nikon Center of Excellence at the Institute for Applied Life Sciences, UMass Amherst, with support from the Massachusetts Life Sciences Center.

BioID and mass spectrometry. BioID was originally developed by Roux et al. (55) and makes use of a promiscuous biotin ligase: the BirA ligase. Samples were prepared as in reference 34. Briefly, iSLK-ORF20$_{STOP}$ cells were seeded in 10-cm plates and reactivated at the same time. Twenty-four hours later, cells were transfected using PolyJet with 5 μg of the ORF20-BirA construct (or mock-BirA control vector), and 50 μM Biotin was added to the medium. The following day, cells were harvested and lysed, and affinity purification was performed using magnetic streptavidin beads (Cell Signaling) overnight at 4°C. Beads were then extensively washed and trypsin digested overnight. Samples were then cleaned up using a C$_{18}$ column, and mass spectral data were obtained at the University of Massachusetts Mass Spectrometry Center using an Orbitrap Fusion mass spectrometer.

Statistical analysis. All results are expressed as means ± standard errors of the means (SEMs) of experiments independently repeated at least three times. Unpaired Student's *t* test was used to evaluate the statistical difference between samples. Significance was evaluated with *P* values and represented as follows: *, $P < 0.05$; **, $P < 0.01$; ***, $P < 0.001$; ns, nonsignificant.

SUPPLEMENTAL MATERIAL

Supplemental material is available online only.

SUPPLEMENTAL FILE 1, DOCX file, 0.2 MB.

SUPPLEMENTAL FILE 2, XLSX file, 0.2 MB.

REFERENCES

1. Purushothaman P, Uppal T, Verma SC. 2015. Molecular biology of KSHV lytic reactivation. Viruses 7:116–153. https://doi.org/10.3390/v7010116.

2. Dupin N, Fisher C, Kellam P, Ariad S, Tulliez M, Franck N, van Marck E, Salmon D, Gorin I, Escande J-P, Weiss RA, Alitalo K, Boshoff C. 1999. Distribution of human herpesvirus-8 latently infected cells in Kaposi's sarcoma, multicentric Castleman's disease, and primary effusion lymphoma. Proc Natl Acad Sci U S A 96:4546–4551. https://doi.org/10.1073/pnas.96.8.4546.

3. Ganem D. 2007. Chapter 56. KSHV-induced oncogenesis. *In* Arvin A, Campadelli-Fiume G, Mocarski E, Moore PS, Roizman B, Whitley R, Yamanishi K (ed), Human herpesviruses. Cambridge University Press, Cambridge, United Kingdom.

4. Greene W, Kuhne K, Ye F, Chen J, Zhou F, Lei X, Gao S-J. 2007. Molecular biology of KSHV in relation to AIDS-associated oncogenesis, p 69–127. *In* Meyers C (ed), Cancer treatment and research, vol 133. Springer, Boston, MA.

5. Fields BN, Knipe DM, Howley PM. 1996. Fields virology. Lippincott-Raven Publishers, Philadelphia, PA.

6. Lin CL, Li H, Wang Y, Zhu FX, Kudchodkar S, Yuan Y. 2003. Kaposi's sarcoma-associated herpesvirus lytic origin (*ori-Lyt*)-dependent DNA replication: identification of the *ori-Lyt* and association of K8 bZip protein with the origin. J Virol 77:5578–5588. https://doi.org/10.1128/JVI.77.10.5578-5588.2003.

7. Nicholas J, Zong J-C, Alcendor DJ, Ciufo DM, Poole LJ, Sarisky RT, Chiou C-J, Zhang X, Wan X, Guo H-G, Reitz MS, Hayward GS. 1998. Novel organizational features, captured cellular genes, and strain variability within the genome of KSHV/HHV8. J Natl Cancer Inst Monogr 1998:79–88. https://doi.org/10.1093/oxfordjournals.jncimonographs.a024179.

8. AuCoin DP, Colletti KS, Cei SA, Papousková I, Tarrant M, Pari GS. 2004. Amplification of the Kaposi's sarcoma-associated herpesvirus/human herpesvirus 8 lytic origin of DNA replication is dependent upon a *cis*-acting AT-rich region and an ORF50 response element and the *trans*-acting factors ORF50 (K-Rta) and K8 (K-bZIP). Virology 318:542–555. https://doi.org/10.1016/j.virol.2003.10.016.

9. Cousins E, Nicholas J. 2014. Molecular biology of human herpesvirus 8: novel functions and virus-host interactions implicated in viral pathogenesis and replication, p 227–268. *In* Chang M, Jeang KT (ed), Viruses and human cancer. Recent results in cancer research, vol 193. Springer, Berlin, Germany. https://doi.org/10.1007/978-3-642-38965-8_13.

10. Chan SR, Chandran B. 2000. Characterization of human herpesvirus 8 ORF59 protein (PF-8) and mapping of the processivity and viral DNA polymerase-interacting domains. J Virol 74:10920–10929. https://doi.org/10.1128/jvi.74.23.10920-10929.2000.

11. Lin K, Dai CY, Ricciardi RP. 1998. Cloning and functional analysis of Kaposi's sarcoma-associated herpesvirus DNA polymerase and its processivity factor. J Virol 72:6228–6232. https://doi.org/10.1128/JVI.72.7.6228-6232.1998.

12. Chan SR, Bloomer C, Chandran B. 1998. Identification and characterization of human herpesvirus-8 lytic cycle-associated ORF 59 protein and the encoding cDNA by monoclonal antibody. Virology 240:118–126. https://doi.org/10.1006/viro.1997.8911.

13. Rossetto CC, Susilarini NK, Pari GS. 2011. Interaction of Kaposi's sarcoma-associated herpesvirus ORF59 with oriLyt is dependent on binding with K-Rta. J Virol 85:3833–3841. https://doi.org/10.1128/JVI.02361-10.

14. McDowell ME, Purushothaman P, Rossetto CC, Pari GS, Verma SC. 2013. Phosphorylation of Kaposi's sarcoma-associated herpesvirus processivity factor ORF59 by a viral kinase modulates its ability to associate with RTA and *ori*Lyt. J Virol 87:8038–8052. https://doi.org/10.1128/JVI.03460-12.

15. Kobiler O, Weitzman MD. 2019. Herpes simplex virus replication compartments: from naked release to recombining together. PLoS Pathog 15:e1007714. https://doi.org/10.1371/journal.ppat.1007714.

16. Wu FY, Ahn JH, Alcendor DJ, Jang WJ, Xiao J, Hayward SD, Hayward GS. 2001. Origin-independent assembly of Kaposi's sarcoma-associated herpesvirus DNA replication compartments in transient cotransfection assays and association with the ORF-K8 protein and cellular PML. J Virol 75:1487–1506. https://doi.org/10.1128/JVI.75.3.1487-1506.2001.

17. Zhong L, Hayward GS. 1997. Assembly of complete, functionally active herpes simplex virus DNA replication compartments and recruitment of associated viral and cellular proteins in transient cotransfection assays. J Virol 71:3146–3160. https://doi.org/10.1128/JVI.71.4.3146-3160.1997.

18. Hollingworth R, Horniblow RD, Forrest C, Stewart GS, Grand RJ. 2017. Localization of double-strand break repair proteins to viral replication compartments following lytic reactivation of Kaposi's Sarcoma-associated herpesvirus. J Virol 91:e00930-17. https://doi.org/10.1128/JVI.00930-17.

19. Schmid M, Speiseder T, Dobner T, Gonzalez RA. 2014. DNA virus replication compartments. J Virol 88:1404–1420. https://doi.org/10.1128/JVI.02046-13.

20. Jacobson JG, Martin SL, Coen DM. 1989. A conserved open reading frame that overlaps the herpes simplex virus thymidine kinase gene is important for viral growth in cell culture. J Virol 63:1839–1843. https://doi.org/10.1128/JVI.63.4.1839-1843.1989.

21. Jacobson JG, Chen SH, Cook WJ, Kramer MF, Coen DM. 1998. Importance of the herpes simplex virus *UL24* gene for productive ganglionic infection in mice. Virology 242:161–169. https://doi.org/10.1006/viro.1997.9012.

22. Nascimento R, Dias JD, Parkhouse RME. 2009. The conserved UL24 family of human alpha, beta and gamma herpesviruses induces cell cycle arrest and inactivation of the cyclinB/cdc2 complex. Arch Virol 154:1143–1149. https://doi.org/10.1007/s00705-009-0420-y.

23. Siew V-K, Duh C-Y, Wang S-K. 2009. Human cytomegalovirus UL76 induces chromosome aberrations. J Biomed Sci 16:107. https://doi.org/10.1186/1423-0127-16-107.

24. Nascimento R, Parkhouse RME. 2007. Murine gammaherpesvirus 68 ORF20 induces cell-cycle arrest in G2 by inhibiting the Cdc2-cyclin B complex. J Gen Virol 88:1446–1453. https://doi.org/10.1099/vir.0.82589-0.

25. Pearson A, Coen DM. 2002. Identification, localization, and regulation of expression of the UL24 protein of herpes simplex virus type 1. J Virol 76:10821–10828. https://doi.org/10.1128/JVI.76.21.10821-10828.2002.

26. Ben Abdeljelil N, Rochette P-A, Pearson A. 2013. The UL24 protein of herpes simplex virus 1 affects the sub-cellular distribution of viral glycoproteins involved in fusion. Virology 444:263–273. https://doi.org/10.1016/j.virol.2013.06.021.

27. Lin S-R, Jiang MJ, Wang H-H, Hu C-H, Hsu M-S, Hsi E, Duh C-Y, Wang S-K. 2013. Human cytomegalovirus UL76 elicits novel aggresome formation via interaction with S5a of the ubiquitin proteasome system. J Virol 87:11562–11578. https://doi.org/10.1128/JVI.01568-13.

28. Bussey KA, Lau U, Schumann S, Gallo A, Osbelt L, Stempel M, Arnold C, Wissing J, Gad HH, Hartmann R, Brune W, Jänsch L, Whitehouse A, Brinkmann MM. 2018. The interferon-stimulated gene product oligoadenylate synthetase-like protein enhances replication of Kaposi's sarcoma-associated herpesvirus (KSHV) and interacts with the KSHV ORF20 protein. PLoS Pathog 14:e1006937. https://doi.org/10.1371/journal.ppat.1006937.

29. Lymberopoulos MH, Pearson A. 2007. Involvement of *UL24* in herpes-simplex-virus-1-induced dispersal of nucleolin. Virology 363:397–409. https://doi.org/10.1016/j.virol.2007.01.028.

30. Lymberopoulos MH, Bourget A, Ben Abdeljelil N, Pearson A. 2011. Involvement of the UL24 protein in herpes simplex virus 1-induced dispersal of B23 and in nuclear egress. Virology 412:341–348. https://doi.org/10.1016/j.virol.2011.01.016.

31. Pearson A, Bourget A, Ben Abdeljelil N, Lymberopoulos MH. 2011. Role of the viral protein UL24 in nucleolar modifications induced by herpes simplex virus 1. BMC Proc 5:P102. https://doi.org/10.1186/1753-6561-5-S1-P102.

32. Yoo SM, Zhou F-C, Ye F-C, Pan H-Y, Gao S-J. 2005. Early and sustained expression of latent and host modulating genes in coordinated transcriptional program of KSHV productive primary infection of human primary endothelial cells. Virology 343:47–64. https://doi.org/10.1016/j.virol.2005.08.018.

33. Brulois KF, Chang H, Lee AS-Y, Ensser A, Wong L-Y, Toth Z, Lee SH, Lee H-R, Myoung J, Ganem D, Oh T-K, Kim JF, Gao S-J, Jung JU. 2012. Construction and manipulation of a new Kaposi's sarcoma-associated herpesvirus bacterial artificial chromosome clone. J Virol 86:9708–9720. https://doi.org/10.1128/JVI.01019-12.

34. Roux KJ, Kim DI, Burke B, May DG. 2018. BioID: a screen for protein-protein interactions. Curr Protoc Protein Sci 91:19.23.1–19.23.15. https://doi.org/10.1002/cpps.51.

35. Dembowski JA, DeLuca NA. 2015. Selective recruitment of nuclear factors to productively replicating herpes simplex virus genomes. PLoS Pathog 11:e1004939. https://doi.org/10.1371/journal.ppat.1004939.

36. Muller M, Hutin S, Marigold O, Li KH, Burlingame A, Glaunsinger BA. 2015. A ribonucleoprotein complex protects the interleukin-6 mRNA from degradation by distinct herpesviral endonucleases. PLoS Pathog 11:e1004899. https://doi.org/10.1371/journal.ppat.1004899.

37. Atari N, Rajan KS, Chikne V, Cohen-Chalamish S, Orbaum O, Jacob A, Kalt I, Michaeli S, Sarid R. 15 May 2020. Lytic reactivation of the Kaposi's sarcoma-associated herpesvirus (KSHV) is accompanied by major nucleolar alterations. bioRxiv https://doi.org/10.1101/2020.05.15.097808.

38. Diekmann U. 2019. Characterisation of the KSHV protein ORF20 and its role in innate immunity. Thesis. Technical University Carolo-Wilhelmina, Braunschweig, Germany. https://doi.org/10.24355/dbbs.084-201903041425-0.

39. Li D, Fu W, Swaminathan S. 2018. Continuous DNA replication is required for late gene transcription and maintenance of replication compartments in gammaherpesviruses. PLoS Pathog 14:e1007070. https://doi.org/10.1371/journal.ppat.1007070.

40. Taylor TJ, McNamee EE, Day C, Knipe DM. 2003. Herpes simplex virus replication compartments can form by coalescence of smaller compartments. Virology 309:232–247. https://doi.org/10.1016/S0042-6822(03)00107-7.

41. Kobiler O, Brodersen P, Taylor MP, Ludmir EB, Enquist LW. 2011. Herpesvirus replication compartments originate with single incoming viral genomes. mBio 2:e002478-11. https://doi.org/10.1128/mBio.00278-11.

42. Chang L, Godinez WJ, Kim I-H, Tektonidis M, de Lanerolle P, Eils R, Rohr K, Knipe DM. 2011. Herpesviral replication compartments move and coalesce at nuclear speckles to enhance export of viral late mRNA. Proc Natl Acad Sci U S A 108:E136–W144. https://doi.org/10.1073/pnas.1103411108.

43. Leiva-Torres GA, Rochette P-A, Pearson A. 2010. Differential importance of highly conserved residues in UL24 for herpes simplex virus 1 replication *in vivo* and reactivation. J Gen Virol 91:1109–1116. https://doi.org/10.1099/vir.0.017921-0.

44. Song MJ, Hwang S, Wong WH, Wu T-T, Lee S, Liao H-I, Sun R. 2005. Identification of viral genes essential for replication of murine gamma-herpesvirus 68 using signature-tagged mutagenesis. Proc Natl Acad Sci U S A 102:3805–3810. https://doi.org/10.1073/pnas.0404521102.

45. Knizewski L, Kinch L, Grishin NV, Rychlewski L, Ginalski K. 2006. Human herpesvirus 1 *UL24* gene encodes a potential PD-(D/E)XK endonuclease. J Virol 80:2575–2577. https://doi.org/10.1128/JVI.80.5.2575-2577.2006.

46. Bertrand L, Leiva-Torres GA, Hyjazie H, Pearson A. 2010. Conserved residues in the UL24 protein of herpes simplex virus 1 are important for dispersal of the nucleolar protein nucleolin. J Virol 84:109–118. https://doi.org/10.1128/JVI.01428-09.

47. Mendez AS, Vogt C, Bohne J, Glaunsinger BA. 2018. Site specific target binding controls RNA cleavage efficiency by the Kaposi's sarcoma-associated herpesvirus endonuclease SOX. Nucleic Acids Res 46:11968–11979. https://doi.org/10.1093/nar/gky932.

48. Glaunsinger B, Chavez L, Ganem D. 2005. The exonuclease and host shutoff functions of the SOX protein of Kaposi's sarcoma-associated herpesvirus are genetically separable. J Virol American Society for Microbiology 79:7396–7401. https://doi.org/10.1128/JVI.79.12.7396-7401.2005.

49. Bagnéris C, Briggs LC, Savva R, Ebrahimi B, Barrett TE. 2011. Crystal structure of a KSHV-SOX-DNA complex: insights into the molecular mechanisms underlying DNase activity and host shutoff. Nucleic Acids Res 39:5744–5756. https://doi.org/10.1093/nar/gkr111.

50. Uppal T, Meyer D, Agarwal A, Verma SC. 2019. The DNase activity of Kaposi's sarcoma-associated herpesvirus SOX protein serves an important role in viral genome processing during lytic replication. J Virol 93:e01983-18. https://doi.org/10.1128/JVI.01983-18.

51. Schumacher AJ, Mohni KN, Kan Y, Hendrickson EA, Stark JM, Weller SK. 2012. The HSV-1 exonuclease, UL12, stimulates recombination by a single strand annealing mechanism. PLoS Pathog 8:e1002862. https://doi.org/10.1371/journal.ppat.1002862.

52. Myoung J, Ganem D. 2011. Generation of a doxycycline-inducible KSHV producer cell line of endothelial origin: maintenance of tight latency with efficient reactivation upon induction. J Virol Methods 174:12–21. https://doi.org/10.1016/j.jviromet.2011.03.012.

53. Nakamura H, Lu M, Gwack Y, Souvlis J, Zeichner SL, Jung JU. 2003. Global changes in Kaposi's sarcoma-associated virus gene expression patterns following expression of a tetracycline-inducible Rta transactivator. J Virol 77:4205–4220. https://doi.org/10.1128/jvi.77.7.4205-4220.2003.

54. Davis ZH, Verschueren E, Jang GM, Kleffman K, Johnson JR, Park J, Von Dollen J, Maher MC, Johnson T, Newton W, Jäger S, Shales M, Horner J, Hernandez RD, Krogan NJ, Glaunsinger BA. 2015. Global mapping of herpesvirus-host protein complexes reveals a transcription strategy for late genes. Mol Cell 57:349–360. https://doi.org/10.1016/j.molcel.2014.11.026.

55. Roux KJ, Kim DI, Raida M, Burke B. 2012. A promiscuous biotin ligase fusion protein identifies proximal and interacting proteins in mammalian cells. J Cell Biol 196:801–810. https://doi.org/10.1083/jcb.201112098.